Aquaculture 577 (2023) 739970

Contents lists available at ScienceDirect

Aquaculture

journal homepage: www.elsevier.com/locate/aquaculture

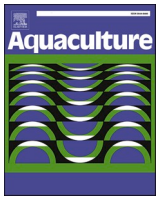

# Formation of asymmetric body color in the caudal fin of common carp (*Cyprinus carpio*)

Guangjing Zhang [a,b,1], Lingqian Tang [a,b,1], Jing Huang [a,b], Yujiao Wang [a,b], Haitao Wang [a,b], Yunpeng Fan [a,b], Xiudan Yuan [a,b], Wenbin Liu [a,b], Liangyue Peng [a,b], Jinhui Liu [a,b,*], Yamei Xiao [a,b,*]

[a] State Key Laboratory of Developmental Biology of Freshwater Fish, Hunan Normal University, Changsha 410081, China
[b] College of Life Sciences, Hunan Normal University, Changsha 410081, China

ARTICLE INFO

*Keywords:*
*Cyprinus carpio*
Caudal fin
Erythrophore
Carotenoid
*bco2a* gene

ABSTRACT

Color pattern is one of the most important characteristics of species, which plays essential roles in reproduction, adaptability, and even survival. The adult caudal fin of common carp (*Cyprinus carpio*) has an asymmetrical distribution of body color, with the dorsal lobe (DL) being dark-gray and the ventral lobe (VL) being red. This study first investigates the cytological basis of forming such an asymmetric distribution by observing the component of pigment cells and exploring the early development of the body color, combined with adult caudal fin regeneration experiments in the common carp. In terms of the distribution feature and the number of pigment cells, differences between the DL and the VL are demonstrated, especially with respect to their erythrophores. Abundant lipid droplets and carotenoid droplets are observed in the VL, conforming to the distribution of erythrophores. Analysis of the gene expression profiles indicates that there are highly expressed levels of carotenoid deposition and lipid droplets transport genes, such as *scarb* and *plin6*. In contrast, the gene expression levels of the β-carotene dioxygenase (*bco*) family are significantly down-regulated in the VL. In addition, knocking down of the *bco2a* gene expression level causes a significant increment of erythrophores. It is concluded that the directed accumulation of lipid droplets and carotenoid particles is the reason for the asymmetric distribution of red color in the caudal fin of common carp.

## 1. Introduction

Body color is one of the important phenotypic traits in animals, controlled by basic pigment cells, such as melanocytes, xanthophores, erythrophores and iridocytes (Kimura et al., 2014; Zhang et al., 2017; Vitt et al., 2022). Melanocytes contains a large amount of melanin, making the body appear black. As the most common type of pigment cells in animals, biosynthesis of the melanin, melanocyte differentiation and cell migration are associated with regulation of >200 genes (Yamaguchi and Hearing, 2014; Shosuke and Wakamatsu, 1998; Haage and Tanentzapf, 2023).

The other body colors, yellow, orange and red, were related with the pigment cells of xanthophores and erythrophores. The morphology and chemical composition of these pigment cells were basically similar, consisting of carotenoids and pteridines (Grether et al., 2004; Sefc et al., 2014; Wang et al., 2021). In particular, the xanthophores contained a large amount of pteridines, while the erythrophore was comprised of abundant carotenoids (Djurdjevič et al., 2015; Wang et al., 2021). However, up to now, there is little understanding of the developmental regulation mechanisms of the above mentioned pigment cells (Chen et al., 2021; Sušnik et al., 2022).

Among *Cyprinidae*, there are many important and colorful ornamental fish, such as koi (*Cyprinus carpio haematopterus*) and goldfish (*Carassius auratus linnaeus*). The common carp (*Cyprinus carpio*) is a kind of significant freshwater fish in Asia and possess a symmetrical tail which extends beyond the end of the vertebral column, as in majority of the bony fishes. The adult caudal fin of common carp had an asymmetrical distribution of body color, with the dorsal lobe (DL) being dark-gray and the ventral lobe (VL) being red. In this research, through cytological observation, regeneration tests and transcriptome analysis,

* Corresponding authors at: State Key Laboratory of Developmental Biology of Freshwater Fish, Hunan Normal University, Changsha 410081, China.
*E-mail addresses:* jinhuiliu0731@hunnu.edu.cn (J. Liu), yameix@hunnu.edu.cn (Y. Xiao).
[1] These authors have contributed equally to this work.

https://doi.org/10.1016/j.aquaculture.2023.739970
Received 18 May 2023; Received in revised form 31 July 2023; Accepted 2 August 2023
Available online 4 August 2023

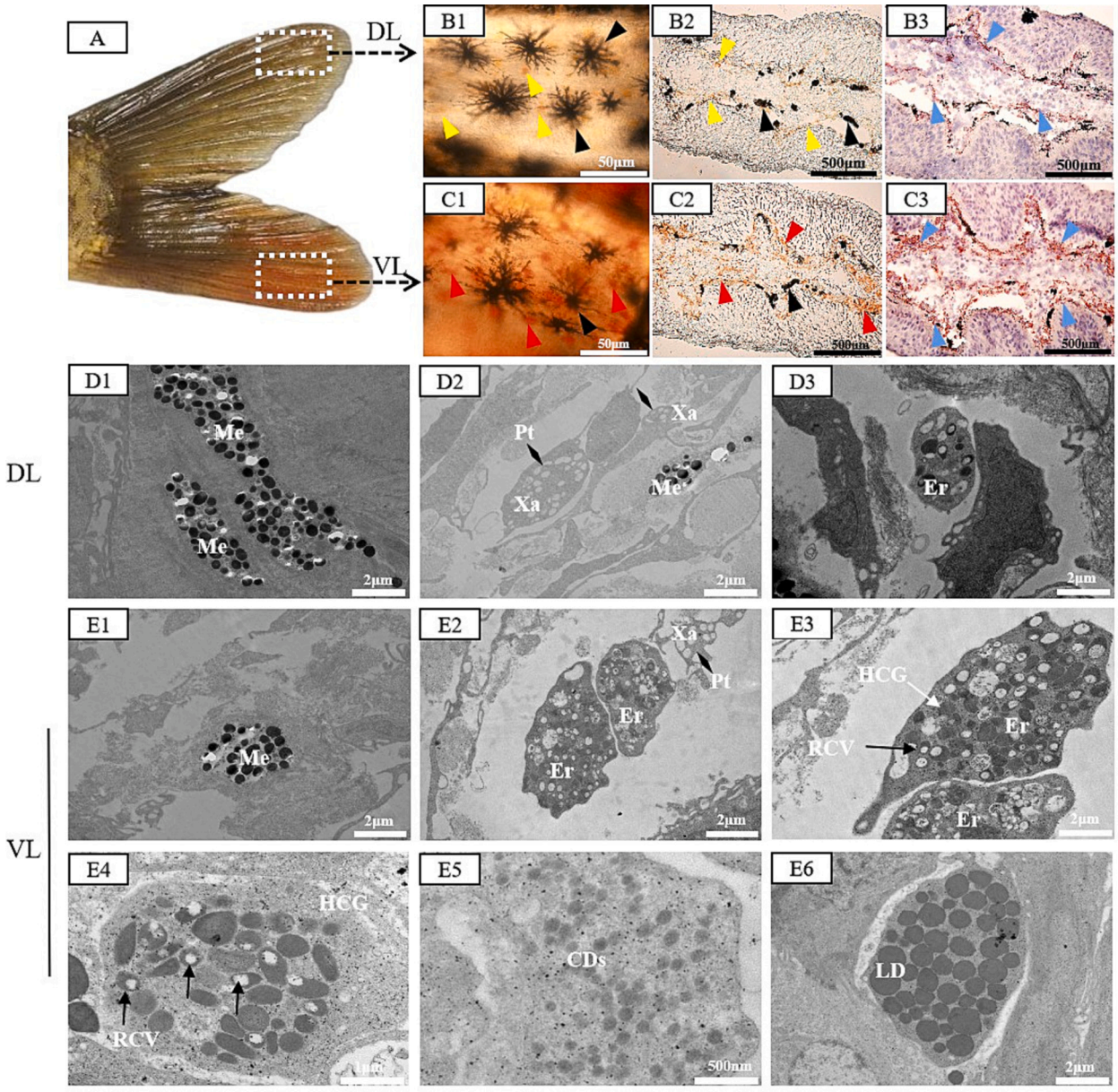


**Fig. 1.** Cytological observation on distribution of body colors in common carp caudal fin.
(A): Different body colors of the dorsal lobe (DL) and ventral lobe (VL). (B1-B3, C1-C3): Results of optical microscopy observation (B1, C1) and the frozen section of pigment cells (B2, C2) of the DL (B1-B3) and VL (C1-C3) . B3 and C3: oil-red staining of the DL and VL; The black triangles refer to melanocytes, the yellow triangles refer to xanthophores, the red triangle refers to erythrophores, and the blue triangles refer to lipids. (D1-D3, E1-E6) The ultra-structures of pigment cells in DL and VL. Me: Melanin; Xa: xanthophore; Pt: Pterinosome; Er: Erythrophore; RCV: Ring Carotenoid vesicle; HCG: Homogenous carotenoid granule; CDs: Carotenoid Droplet; LD: Lipid Droplet. The black diamond-shaped arrow refers to Pt; The black arrow refers to RCV; The white arrow refers to HCG. (For interpretation of the references to color in this figure legend, the reader is referred to the web version of this article.)

we attempt to explore the formation and the regulation mechanism of such an asymmetric distribution feature.

## 2. Materials and methods

### 2.1. Ethics statement

All experimental procedures involving fish were approved by the Institutional Animal Care and Use Committee of Hunan Normal University. Procedures were conducted following the regulations of the Administration of Affairs Concerning Experimental Animals for the Science and Technology Bureau of China.

### 2.2. Fish

Common carp (*Cyprinus carpio*), red koi carp (*Cyprinus carpio* var. *koi*), black koi carp (*Cyprinus carpio var. koi*), red crucian carp (*Carassius auratus var.*), Carassius cuvier (*Carassius auratus cuvieri*), and zebrafish (*Danio rerio*) were maintained at the State Key Laboratory of Developmental Biology of Freshwater Fish, Hunan Normal University.

### 2.3. Histological and ultrathin sectioning

For optical microscopic observation, pieces of caudal fin were surgically excised from fish. Washed three times with 1% PBS (Phosphate buffer saline), then put on a glass slide, covered with a cover slip and observed under a microscope.

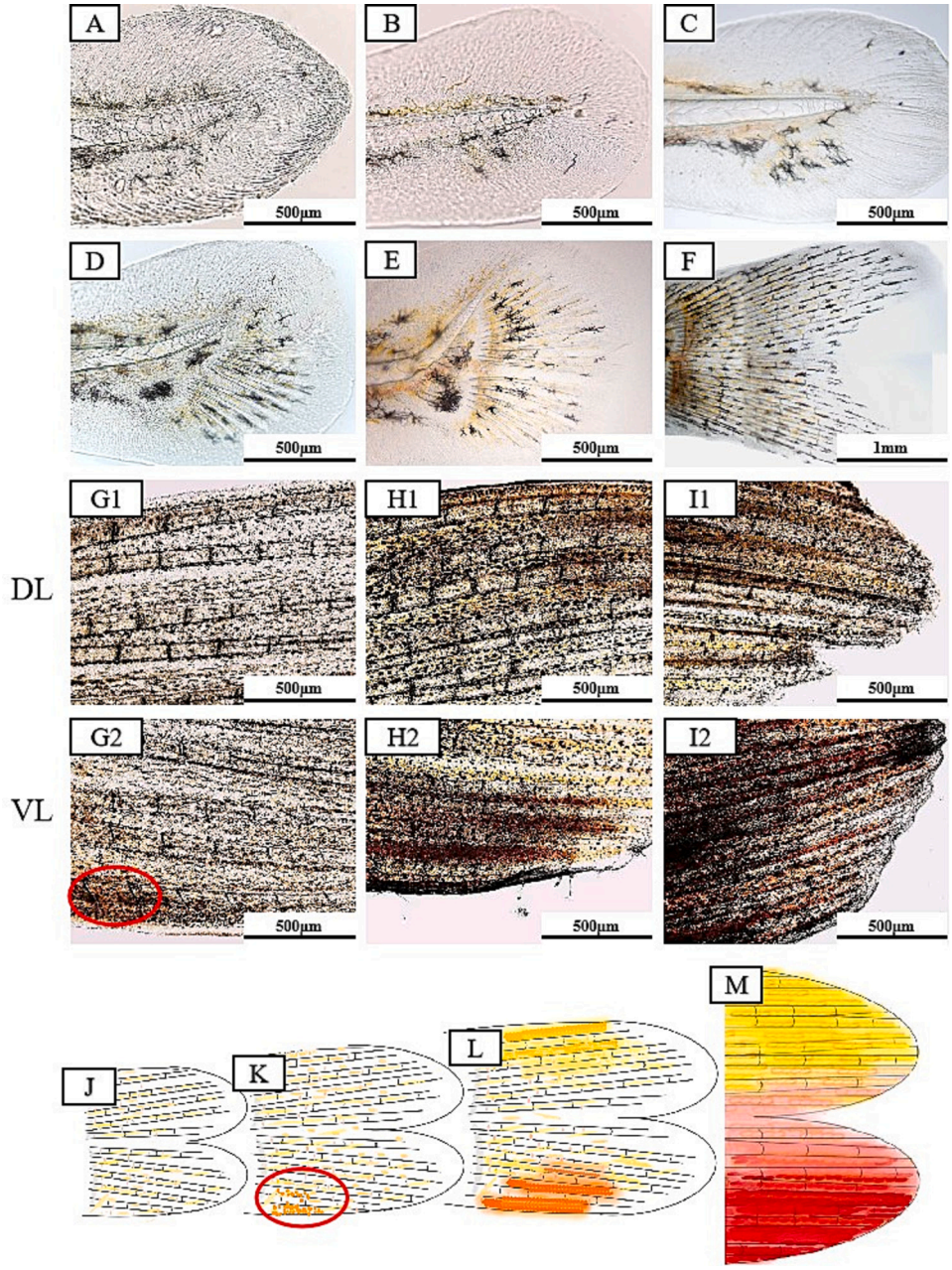


**Fig. 2.** Cytological observation on the formation of body colors in the common carp caudal fin.
(A-F): Caudal fins of 1-, 4-, 7-, 10-, 15-, and 30-day post-hatching (dph) common carps. (G1-G2): The dorsal lobe (DL) and the ventral lobe (VL) of the 45 dph common carp. (H1−H2): The DL and VL of the 2-month-old common carp. (I1-I2): The DL and VL of the 3-month-old common carp. (J-M): Migration simulation diagram of xanthophores (shown by yellow) and erythrophores (shown by red) in the caudal fin during ontogeny. The red dotted circle refers to the boundary where the erythrophores start to appear. (For interpretation of the references to color in this figure legend, the reader is referred to the web version of this article.)

For the ultrastructure observation, small pieces of the caudal fins were fixed at 4 °C in 3% glutaraldehyde solution for 120 min. Washed them three times with 0.2 mol/L phosphoric acids buffer, then they were treated with 1% $O_SO_4$ for 2–3 h. After dehydration through an ethanol series, the specimens were embedded in Epon812 resin (TAAB, USA). Ultrathin slices of the samples about 60 nm were made by ultramicrotome (Germany, Leica EM UC7). Then, the sections were doubly stained with uranyl acetate and lead citrate and were examined by electron microscope (Japan, HT7800).

### 2.4. Oil-red staining

Pieces of the caudal fin were soaked in an optimum cutting temperature compound embedding solution, placed in liquid nitrogen and stored at −80 °C. A section of 10 μm in thickness was obtained in a Leica CM3050S Frozen Micotome. Then, they were soaked in PBS for 10 min, following 60% isopropyl alcohol for 5 min. The oil-red was stained for 15 min without light, and 60% isopropyl alcohol was toned for 1 min. After washing them with pure water, these caudal fin tissues were stained with hematoxylin for 5 min.

### 2.5. Sequencing and analysis

Fresh fin tissues were collected from the DL and VL of the 12-month-old common carp. Two independent biological replicates were used in each group. All the samples were stored at −80 °C.

They were double-ended sequenced using Illumina Novaseq™ 6000 (LC Bio-Technology CO., Ltd. Hangzhou, China) in PE150 sequencing mode according to standard procedures. Quality controls of the plane raw data were performed with Fastp (https://github.com/OpenGene/fastp) software. The StringTie software (https://ccb.jhu.edu/software/hisat2) was used to obtain the transcription of the assembly, and by the calculation method of FPKM, the expressed levels of all genes in each sample were provided. Then, the R package edgeR (htt

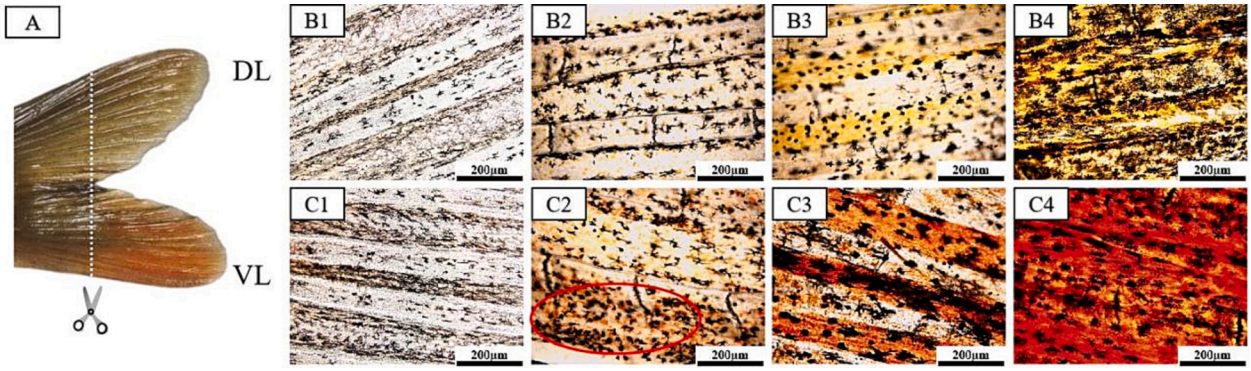


**Fig. 3.** Cytological observation on body colors by regeneration test of caudal fin in common carp.
(A): Regeneration test of tail fins. The white dotted line refers to the shear position. (B1-B4, C1-C4): Cytological observation of the regenerated dorsal lobe (DL) and ventral lobe (VL). The red dotted circle refers to the boundary where erythrophores start to appear. (For interpretation of the references to color in this figure legend, the reader is referred to the web version of this article.)

ps://bioconductor.org/packages/release/bioc/html/edgeR.html) was used to analyze the differences of the expressed levels among the genes, including the fold change >2 or the fold change <0.5. And, *p-value* < 0.05 was defined as a statistically significant difference. Finally, DAVID software (https://david.ncifcrf.gov/) was used to test enrichment of KEGG differences in our gene analysis.

### 2.6. Quantitative real-time PCR (qRT-PCR) analysis

According to the expression levels of the genes, the significantly expressed genes in the DL and the VL of caudal carp fins were screened. The primers were designed using the NCBI Premier (Primer designing tool (nih.gov)), and the presence of dimers was tested with Oligo 7 software, and the primers were synthesized by Qingke Bio (Changsha, China) (Table S1–2). The reference gene for the qRT-PCR was *β-actin*, and the analytical instrument was Quantstudio 5. The results were calculated using the $2^{-\Delta\Delta CT}$ method. Data were presented as the mean values ± standard error of the triplicate measurements' mean (SEM). Statistical significance was tested using the Independent Sample Test in SPSS 20.0 (IBM Corp., Armonk, NY, USA) and was accepted when the *p-value* < *0.05*.

### 2.7. Preparation of bco mutant zebrafish by CRISPR/Cas9

The *bco* mutants were generated by the CRISPR/Cas9 technique in zebrafish. First, the gene target sites were designed using the online tool (CHOPCHOP (uib.no), zifit.partners.org) (Table S3). The *Cas9* mRNA and target sgRNAs were generated by *in vitro* transcription with the T7 kit. The target sgRNA and *Cas9* mRNA were co-injected into single-cell embryos at 20 and 200–300 ng/μL. About 400 fertilized eggs were used for gene editing, and the other 100 were used as the control group.

## 3. Results

### 3.1. Cytological structural differences between dorsal and ventral lobes of caudal fin in common carp

The caudal fin of the common carp, shaped like scissors, belongs to homo-cercal (Fig. 1A). Observation showed that the melanocytes were distributed in the caudal fin of common carp, with a large number of xanthophores visible in the dorsal lobe (DL), and rich erythrophores were found in the ventral lobe (VL) (Fig. 1 B1-2, C1–2). By oil-red staining, a large number of lipid droplets could be seen in the VL, which was significantly more than that in the DL (Fig. 1 B3, C3).

The ultrastructure of the common carp caudal fin demonstrated that melanin and pterinosom in the DL were more than those in the VL (Fig. 1 D1-2, E1–2). The homogenous carotenoid granule and ring carotenoid vesicle were observed in the DL and VL and were more abundant in the VL than those in the DL (Fig. 1 D3, E3–4). Moreover, the VL had lots of carotenoid droplets, apart from a large number of membrane-coated lipid droplets (Fig. 1 E5-6).

### 3.2. Observation on asymmetric body color formation in caudal fin of common carp

In the process of individual growth, melanocytes and xanthophores were observed at the end of the common carp's spine after 1 dph (day post-hatching) and 4 dph, respectively (Fig. 2A, B). Subsequently, a pigment concentration area appeared on the ventral side of the coccyx (Fig. 2C, D). At 15 dph, the caudal fin was still protocercal without forked, and the caudal vertebrae bent towards the dorsal side of the body. Meanwhile, melanocytes and xanthophores migrated radially to the caudal fin (Fig. 2E). At 30 dph, the caudal fin began bifurcation, and the xanthophores following the melanocytes migrated to the tail (Fig. 2F). About 45 dph, the erythrophores started to accumulate at the VL of the forked tail fin (Fig. 2 G1-2, K). The asymmetric body colors in the caudal fin occurred at the 3-month old common carps, with the increased number of erythrophores, which gradually spread towards the tip of the tail fin, maintaining till their adulthood (Fig. 2 H1-2, I1–2, L, M).

To further understand the characteristics of the localized distribution of pigment cells in the tail fin of common carp, the regeneration test of the caudal fin was carried out in adult fish (Fig. 3A). Melanocytes appeared 15 days after surgery, followed by xanthophores and erythrophores one week later in the regenerated caudal fin tissue (Fig. 3 B1-2; C1–2). Unlike xanthophores were evenly distributed in the DL and VL, erythrophores were only limited to the VL of the regenerated tail fin (Fig. 3 B2, C2). One month later, the surgery tail fin was regenerated and still maintained its asymmetrical body color in the caudal fin (Fig. 3 B3-4; C3–4).

### 3.3. Comparative analysis of gene expression profiles in the asymmetric body color of common carp caudal fin

The mRNA transcriptome profiles of DL and VL in common carp's caudal fin were analyzed to obtain about 76,929 transcripts. Between the DL and the VL, a total of 772 genes were significantly differentially expressed, of which 480 (62.18%) were up-regulated and 292 (37.82%) were down-regulated in the DL (Fig. 4A). Analysis of the KEGG pathways revealed that multiple pathways, including the “melanogenesis pathway”, “gap junction pathway”, and “apelin signal pathway”, were enriched in these differentially expressed genes among the DL and the VL (Fig. 4B).

The quantitative analysis results of qRT-PCR showed that the

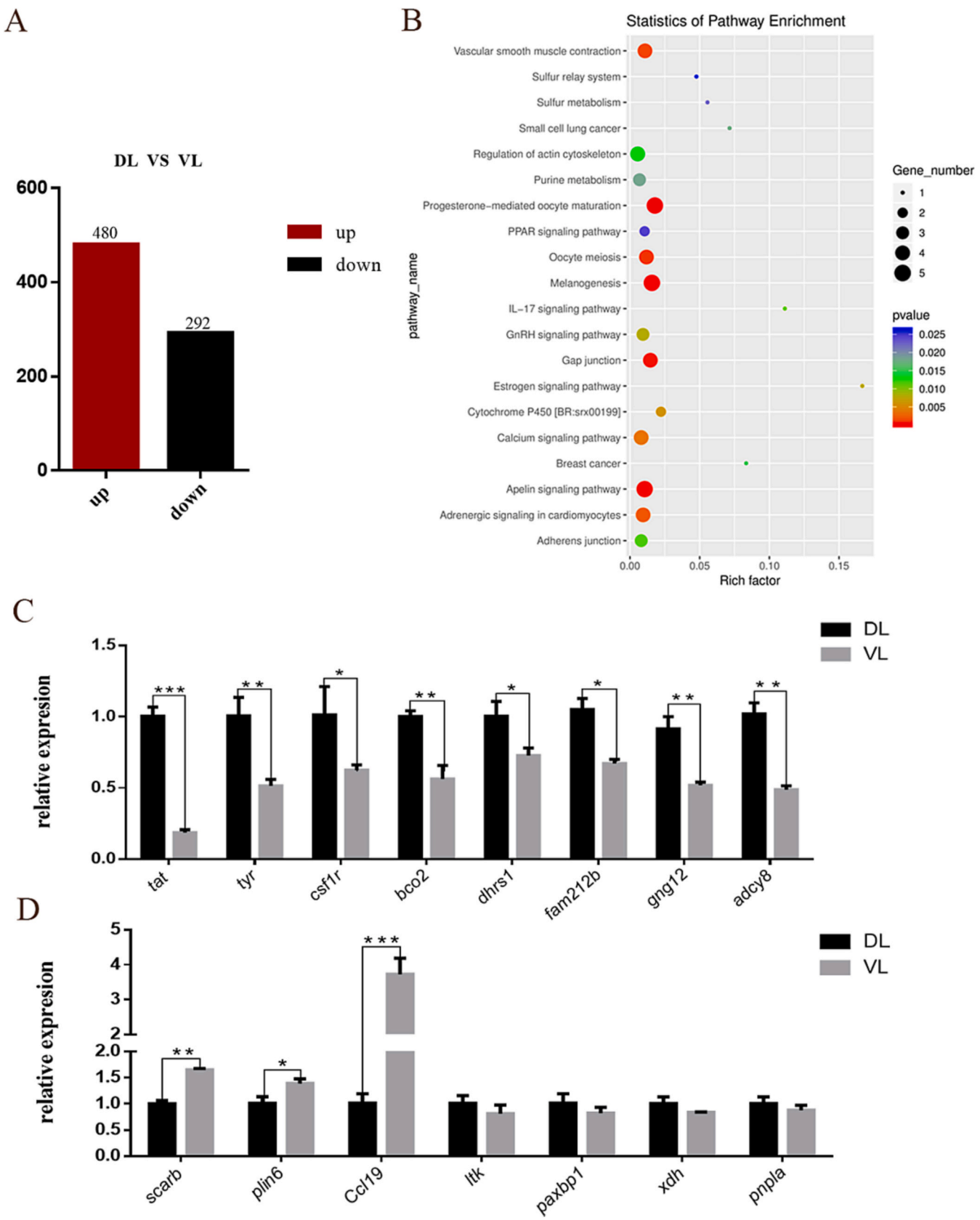


**Fig. 4.** Analysis of gene expression levels in the caudal fin of common carp.
(A) Differential gene expression levels in the dorsal lobe (DL) and the ventral lobe (VL) of the caudal fin of carp. (B) KEGG annotation, functional classification and KEGG enrichment analysis. (C, D): qRT-PCR to detect the expression of pigment-related genes and the part differential genes in the transcriptome. "*": $p < 0.05$; "**": $p < 0.01$; "***": $p < 0.001$. (means ± SD of relative expression; $n = 3$ for each group)

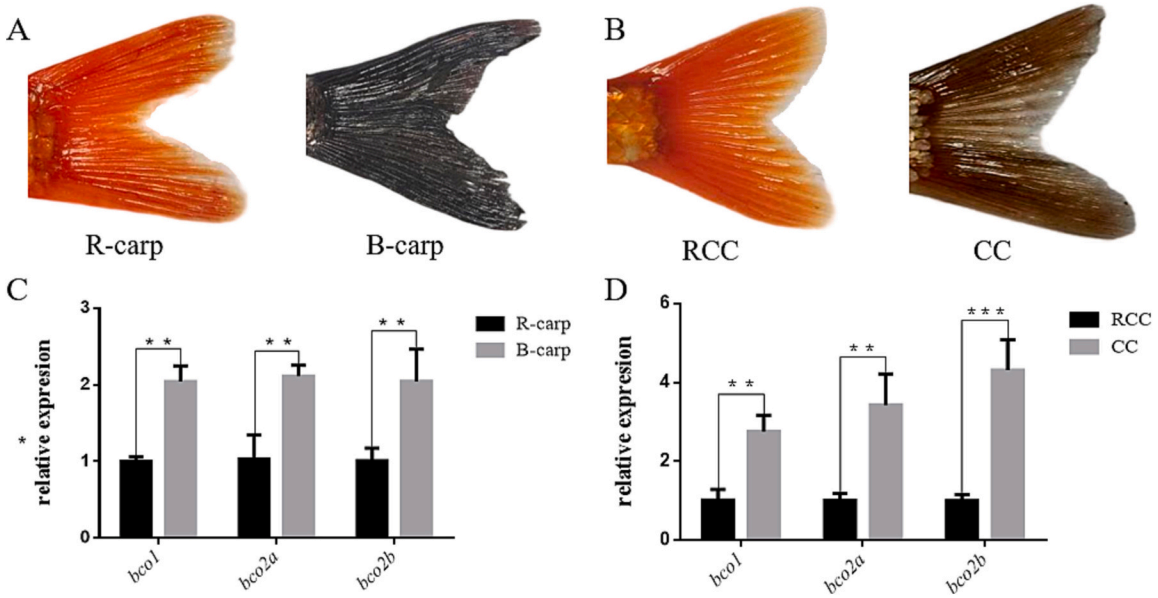


**Fig. 5.** Expression levels of β-carotenoid oxygenase (*bco*) genes in the caudal fins of different body colors.
(A) The caudal fins of red koi carp (R-carp) and black koi carp (B-carp). (B) The caudall fins of red crucian carp (RCC) and carassius cuvier (CC). (C) Expression levels of *bco* genes in the caudal fins of R-carp and B-carp. (D) Expression levels of *bco* genes in the caudal fins of RCC and CC. "*": $p < 0.05$; "**": $p < 0.01$; "***": $p < 0.001$. (means ± SD of relative expression; n = 3 for each group) (For interpretation of the references to color in this figure legend, the reader is referred to the web version of this article.)

expression levels of the melanocyte-related tyrosine metabolism genes (*Tat* and *tyr*), xanthate-related genes (*csf1r*), carotenoid cracking gene (*bco*), and lipid metabolism-related genes (*Dhrs1*, *fam212b*, *gng12* and *Adcy8*) were up-regulated in the DL (Fig. 4C). Meanwhile, expression levels of the carotenoid uptake and storage-related genes, such as *Scarb1*, *plin6* and *Ccl19*, were higher in the VL than those in the DL (Fig. 4D). There were no significant differences of the expression levels with regard to the other genes related with the pigmentation, such as *ltk* (iridocyte-related gene), *paxbp1*, *xdh* (xanthate-related genes) and *pnpla* (Fig. 4D).

### 3.4. Effects of β-carotenoid oxygenase on body color development in fish

It was reported that the β-carotene dioxygenase family genes (*bco1*, *bco2a*, and *bco2b*) played essential roles in carotenoid metabolism (Harrison and Kopec, 2020; Lim et al., 2018). Data of RNA-seq and qRT-PCR indicated that the *bco2* gene was significantly down-regulated in the VL compared to those in the DL (Fig. 4). The expression levels of *bco1*, *bco2a*, and *bco2b* were further analyzed in other different body colors in the caudal fin of carp (red koi carp and black koi carp) (Fig. 5A) and crucian carp (red crucian carp and carassius cuvier) (Fig. 5B). As shown in Fig.5, the expression levels of *bco1*, *bco2a*, and *bco2b* in the red caudal fins were significantly lower than those in the black-gray caudal fins (Fig. 5C, D).

To further confirm the roles of the β-carotenoid oxygenase family genes in body color formation, the *bco1*, *bco2a* and *bco2b* genes were respectively disrupted using the CRISPR/Cas9 technique in zebrafish (Fig. 6A). Compared with the control group, and there was no significant change in the body color of *bco1* or *bco2b* mutants. However, in the *bco2a* mutants, there was a significantly increasing number of erythrophores in the fins and scales (Fig. 6B). The qRT-PCR results showed that in the *bco2a* mutants, the expression level of *bco2a* was down-regulated, while those of *scarb* and *plin6* were significantly up-regulated in the *bco2a* mutants (Fig. 6C).

## 4. Discussion

In this study, cytological observation has found abundant carotenoid particles in the VL, including a large number of the homogenous carotenoid granule (HCG) and the ring carotenoid vesicles (RCV), apart from the carotenoid droplets (CDs). Furthermore, lots of lipid droplets (LD) were consistent with the distribution of erythrophores. The data indicated that the formation of asymmetric red color was closely related to the directed accumulation of the carotenoid particles and the lipid droplets in the caudal fin of common carp. Body colors in animals were generated in the skin and their derivatives (Tanaka, 2001; Shiraki et al., 2010; Vitt et al., 2022). It has been reported that pteridines and carotenoids were the main chemical composition of the erythrophores and xanthophores (Grether et al., 2004; Sefc et al., 2014; Wang et al., 2021). Pteridine is a heterocyclic compound formed by juxtaposing pyrimidine and pyrazine, associating with the *de novo* (BH4) biosynthetic pathway (Nagatsu and Ichinose, 1999; Liang et al., 2022). In *Xiphophorus helleri*, the water-soluble pigments of erythrophores were comprised of pteridine derivatives, including large amounts of drosopterin, isodrosopterin, neodrosopterin and sepiapterin, which were responsible for red pigmentation (Matsumoto, 1965). The water-soluble pteridines are associated with the erythrophores and xanthophores pigmentation. However, the carotenoids were mainly responsible for red coloration (Vissio et al., 2021), which were the lipophilic pigments found in plants, fungi, algae and bacteria (Maoka, 2020). Fish cannot synthesize the carotenoids by themself and often needs to obtain them through food. Generally, after initial digestion by the fish, the carotenoids were first dispersed into the gastrointestinal tract and absorbed into the intestinal epithelial cells by the action of intestinal epithelial transmembrane transport proteins, then they were secreted into the lymph by lipoproteins packed into celiac particles and subsequently into the circulatory system (Pike et al., 2007; Reboul, 2019). Carotenoids transported to the erythrophores and xanthophores existed in various forms, such as RCV, HCG, and CDs (Matsumoto, 1965; Matsui et al., 2003). Since the carotenoids were hydrophobic, they blocked the carotenoid absorption in the aqueous environment of the gastrointestinal tract. Thus, transportation of the carotenoids was associated with lipid metabolism (Castellano et al., 2020; Schmeisser et al., 2021). Different fish had different metabolic capacities for the carotenoids, and the formation mechanism of their body color determined by the carotenoids were often distinct (Liu and Chen, 2008). In this research, the conducted analysis of

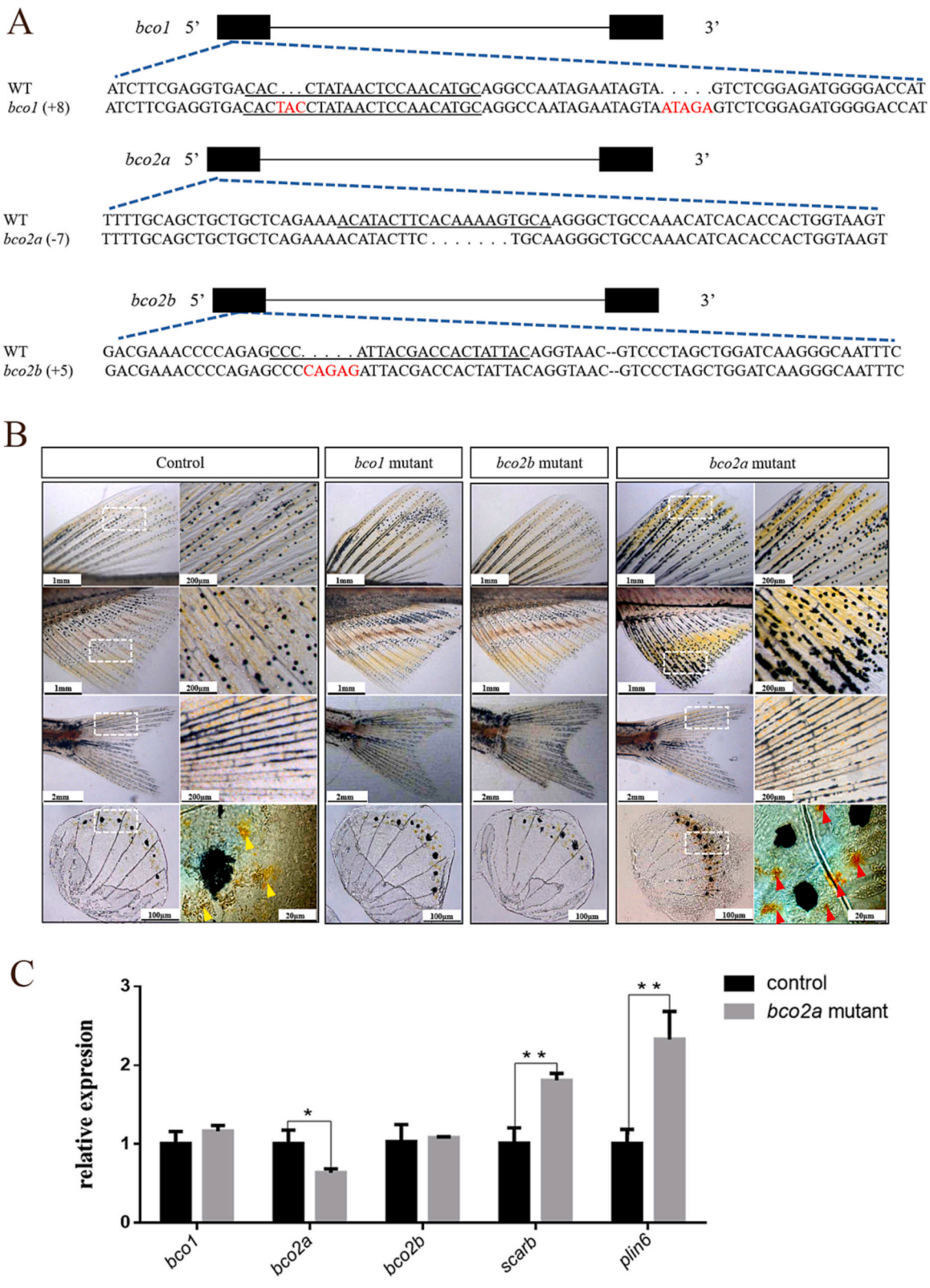


**Fig. 6.** Effects of β-carotenoid oxygenase family gene knockout on the body color development of zebrafish.
(A) Sketch maps of *bco1*, *bco2a* and *bco2b* gene structure of zebrafish and the CRISPR target site. The solid black boxes indicate the exons, and the blue line shows the intron region. The sequence of the CRISPR target site is underlined. The black dots represent the missing bases from the control, and the red bases represent the inserted bases. (B) Observation of pigment in caudal fin and scale of mutant zebrafish. The white dotted box represents the enlarged portion, the yellow triangle refers to xanthophores, the red triangle refers to erythrophores. (C) Expression levels of pigment-related genes in *bco2a* mutant zebrafish. "*": $p < 0.05$; "**": $p < 0.01$; "***": $p < 0.001$. (means ± SD of relative expression; n = 3 for each group) (For interpretation of the references to color in this figure legend, the reader is referred to the web version of this article.)

the carotenoids in the caudal fin of common carp has shown that the components of the neoxanthin were similar between the DL and the VL of the caudal fins (Fig. S1A, C, D). However, the VL had abundant astaxanthin (Fig. S1B—D), not only more than that in the DL, but also more than that in other fish, such as the trout and the salmon (Elmadfa and Majchrzak, 1998). Clearly, the formation and the regulation mechanism causing such differences in astaxanthin both need further investigation.

Several candidate genes related to xanthophore and erythrophore were reported in various organisms. The expression of *csf1ra* was fundamental for xanthophores development in zebrafish and guppy (Kottler et al., 2013; Meng et al., 2021). In *csf1ra* mutants of *Nile tilapia*, xanthophores were reduced in their tails (Lu et al., 2022). *Scarb* was a high-density lipoprotein receptor that might promote carotenoid transport into the pigment cells (Li et al., 2023; Verwilligen-Robin et al., 2013). *Scarb* gene can also selectively absorb beta-carotene, and the upregulation of this gene in the intestinal tract of salmon was related to its reddish meat quality (Reboul et al., 2005). The recessive white canaries (*Serinus canaria*) have little or no carotenoids in their feathers, consistent with a genetic defect in carotenoid uptake due to a mutation in the *Scarb* gene (Toomey et al., 2017). In Oujiang color common carp (*Cyprinus carpio* var. *color*), the disruption of *Scarb* caused dysfunction of carotenoid absorption and transport, resulting in insufficient carotenoid binding and deposition, the original red skin fading into white color (Du et al., 2021). The tissue uptake of carotenoids, the precursor of the antioxidant vitamin A, was impaired in *Scarb* knockout zebrafish, as evidenced by the lack of xanthophores (Sulliman et al., 2021). Perilipin (Plin) constitutes important in LD formation. They were highly expressed in the red/yellow skin, which mediate red/yellow cell pigmentation and trafficking, but not in tissues associated with lipid metabolism. Knockout of *plin6* in zebrafish severely impaired the ability to concentrate carotenoids and prevented tight clustering of carotenoid droplets within carotenoid bodies (Granneman et al., 2017). The C—C motif ligand 19 (*Ccl19*) is a critical regulator of the induction of T cell activation, immune tolerance, and inflammatory responses. But recently, the novel role of CCL19 was revealed to impair lipid metabolism by inhibiting AMPK (Yan et al., 2019; Hayashi et al., 2021).

Moreover, Dehydrogenase/reductase SDR family member 1 (*dhrs1*) and Patatin-like phospholipase domain-containing proteins (*Pnpla*) are involved in lipid droplet formation and metabolism (Zemanová et al., 2019; Taxiarchis et al., 2019). In this research, the expression levels of *csf1r* were down-regulated in the VL, while some of the carotenoid uptake and storage-related genes, such as *Scarb1, plin6, Ccl19* and *dhrs1*, were higher expressed levels in the VL than those of the DL. The transcriptome and qRT-PCR data from the caudal fin of common carp indicated that the differential expressed genes in the caudal fin of carp were enriched in the Apelin signaling pathway, and the red VL in common carp were related to the genes of carotenoid transport and deposition.

β-Carotene-15, 15′-oxygenase (*bco1*) and β-carotene-9′, 10′-oxygenase (*bco2*) can catalyze the decomposition of carotenoids into colorless derivatives. The specific expression of this gene is related to the level of carotenoid intake (Lim et al., 2018). A nonsense mutation in the *bco2* gene was reported to significantly associate with the yellow fat phenotype in sheep (Våge and Boman, 2010). In birds, *bco2* was reported to be essential to turn the orange carotenoid into a colorless carotenoid (Wang et al., 2022). In carotenoid pigmentation in salmon, the *bco2* gene controls a key fitness trait affecting red coloration (Lehnert et al., 2019). The *bco2* gene regulates the degradation degree of carotenoids in the epiderm of these canaries (Gazda et al., 2020). Our results suggest that the genes of the *bco* family were differentially expressed in the caudal fins with different body colors. In the red caudal fins, the expression levels were significantly lower than those in the black-gray caudal fins. To further understand the role of the β-carotenoid oxygenase family genes in the red luteal color formation, we disrupted the *bco1*, *bco2a* and *bco2b* genes using the CRISPR/Cas9 technique in zebrafish. We targeted *bco1* exon1, *bco2a* in exon 1, and *bco2b* in exon 1 within the open reading frame region and downstream of the translation start site to generate *bco1*, *bco2a* and *bco2b* single mutants, respectively. In the *bco2a* mutant, the carotenoids in zebrafish *bco2a* mutant accumulation in the individual caused zebrafish dorsal and anal fin and scales of xanthophores and erythrophores qualitative change. Moreover, the expression of *scarb* and *plin* genes was upregulated in the *bco2a* mutant. These results further confirmed that the *bco2a* gene was essential to the formation of the body color.

The caudal fin of fish has the ability to regenerate. Our previous research has found a distinct light-colored region with less pigment at the heel of caudal fin in the juvenile crucian carp, and argued that this region was a melanocyte progenitor niche (Huang et al., 2017). In this research, the surgically caudal fin could regenerate according to the original pigment pattern in the adult common carp, with the DL being dark-gray and the VL being red (Fig. 3). Moreover, it has been demonstrated that there also existed a light colored region near the base of caudal fin in the juvenile common carp (Fig.2E). It is interesting and valuable to further explore whether this light colored region was involved with the formation of the caudal fin's different color or not.

In conclusion, the conducted investigation in this research indicated that the differential distribution of erythrophores was the primary factor contributing to the formation of asymmetric body coloration in the caudal fins of common carp. The low-level expression of carotenoid degrading genes (*bco*) and the high-level expression of carotenoid deposition (*scarb*) and lipid droplet transport (*plin6*) genes played essential roles in the carotenoid accumulation and regulation of forming the body color in fish.

## CRediT authorship contribution statement

**Guangjing Zhang:** Investigation, Data curation, Formal analysis, Writing – original draft. **Lingqian Tang:** Investigation, Data curation, Formal analysis, Writing – original draft. **Jing Huang:** Investigation, Methodology. **Yujiao Wang:** Formal analysis. **Haitao Wang:** Formal analysis. **Yunpeng Fan:** Formal analysis. **Xiudan Yuan:** Formal analysis. **Wenbin Liu:** Writing – review & editing. **Liangyue Peng:** Writing – review & editing. **Jinhui Liu:** Conceptualization, Project administration. **Yamei Xiao:** Conceptualization, Project administration.

## Declaration of Competing Interest

The authors declare that they have no competing interests.

## Data availability

Data will be made available on request.

## Acknowledgements

This study was supported by the National Natural Science Foundation of China (31802284, 31472272).

## References

Castellano, J.M., Espinosa, J.M., Perona, J.S., 2020. Modulation of lipid transport and adipose tissue deposition by small lipophilic compounds. Front. Cell. Dev. Biol. 8, 555359.

Chen, J., Li, S., Li, C., 2021. Mechanisms of melanocyte death in vitiligo. Med. Res. Rev. 41 (2), 1138–1166.

Djurdjević, I., Kreft, M.E., Sušnik, B.S., 2015. Comparison of pigment cell ultrastructure and organization in the dermis of marble trout and brown trout, and first description of erythrophore ultrastructure in salmonids. J. Anat. 227 (5), 583–595.

Du, J.X., Chen, H.L., Mandal, B.K., Wang, J., Shi, Z.Y., Lu, G.Q., Wang, C.H., 2021. HDL receptor/scavenger receptor B1-Scarb1 and Scarb1-like mediate the carotenoid-based red coloration in fish. Aquaculture 545, 737208.

Elmadfa, I., Majchrzak, D., 1998. Carotinoide and vitamin a in fischproben. Z. Ernahrungswiss. 37 (2), 207–210.

Gazda, M.A., Araújo, P.M., Lopes, R.J., Toomey, M.B., Andrade, P., Afonso, S., Marques, C., Nunes, L., Pereira, P., Trigo, S., Hill, G.E., Corbo, J.C., Carneiro, M.,

2020. A genetic mechanism for sexual dichromatism in birds. Science 368 (6496), 1270–1274.
Granneman, J.G., Kimler, V.A., Zhang, H., Ye, X., Luo, X., Postlethwait, J.H., Thummel, R., 2017. Lipid droplet biology and evolution illuminated by the characterization of a novel perilipin in teleost fish. Elife. 6, e21771.
Grether, G.F., Kolluru, G.R., Nersissian, K., 2004. Individual colour patches as multicomponent signals. Biol. Rev. Camb. Philos. Soc. 79 (3), 583–610.
Haage, A., Tanentzapf, G., 2023. Analysis of integrin-dependent melanoblast migration during development. Methods Mol. Biol. 2608, 207–221.
Harrison, E.H., Kopec, R.E., 2020. Enzymology of vertebrate carotenoid oxygenases. Biochim. Biophys. Acta Mol. Cell Biol. Lipids 1865 (11), 158653.
Hayashi, M., Iwashita, M., Nishimura, Y., Shinjo, T., Sano, T., Yamashita, A., Fukuda, T., Sanui, T., Asano, T., Nishimura, F., 2021. Adipose-specific C-C motif chemokine ligand (CCL) 19 overexpression drives the mice to both insulin resistance and weight gain. BMJ Open Diabetes Res. Care 9 (1), e001871.
Huang, Y., Luo, Y., Liu, J., Gui, S., Wang, M., Liu, W., Peng, L., Xiao, Y., 2017. A light-colored region of caudal fin: a niche of melanocyte progenitors in crucian carp (*Cyprinus carpio* L.). Cell Biol. Int. 41 (1), 42–50.
Kimura, T., Nagao, Y., Hashimoto, H., Yamamoto-Shiraishi, Y., Yamamoto, S., Yabe, T., Takada, S., Kinoshita, M., Kuroiwa, A., Naruse, K., 2014. Leucophores are similar to xanthophores in their specification and differentiation processes in medaka. Proc. Natl. Acad. Sci. U. S. A. 111 (20), 7343–7348.
Kottler, V.A., Fadeev, A., Weigel, D., Dreyer, C., 2013. Pigment pattern formation in the guppy, *Poecilia reticulata*, involves the *Kita* and *Csf1ra* receptor tyrosine kinases. Genetics 194 (3), 631–646.
Lehnert, S.J., Christensen, K.A., Vandersteen, W.E., Sakhrani, D., Pitcher, T.E., Heath, J. W., Koop, B.F., Heath, D.D., Devlin, R.H., 2019. Carotenoid pigmentation in salmon: variation in expression at BCO2-l locus controls a key fitness trait affecting red coloration. Proc. Biol. Sci. 286 (1913), 20191588.
Li, B., George, E.W., Vachali, P., Chang, F.Y., Gorusupudi, A., Arunkumar, R., Giauque, N.A., Wan, Z., Frederick, J.M., Bernstein, P.S., 2023. Mechanism for the selective uptake of macular carotenoids mediated by the HDL cholesterol receptor SR-BI. Exp. Eye Res. 229, 109429.
Liang, D., Shu, R., Jiang, S., Yang, L., Wang, Y., Zhao, Y., Cai, Y., Xie, R., Meng, Y., 2022. Identification and functional analysis of carbonyl reductases related to tetrahydrobiopterin synthesis in the silkworm, *Bombyx mori*. Insect Mol. Biol. 31 (4), 403–416.
Lim, J.Y., Liu, C., Hu, K.Q., Smith, D.E., Wang, X.D., 2018. Ablation of carotenoid cleavage enzymes (BCO1 and BCO2) induced hepatic steatosis by altering the farnesoid X receptor/miR-34a/sirtuin 1 pathway. Arch. Biochem. Biophys. 654, 1–9.
Liu, X.D., Chen, Z.Z., 2008. Observation of pigmented cells and analysis of carotenoid components in skin of discoloured angelfish. J. Shanghai Fisheries U. 03, 339–343.
Lu, B.Y., Wang, C.X., Liang, G.Y., Xu, M.M., Kocher, T.D., Sun, L.N., Wang, X.D., 2022. Generation of ornamental Nile tilapia with distinct gray and black body color pattern by *csf1ra* mutation. Aquac. Rep. 23, 101077.
Maoka, T., 2020. Carotenoids as natural functional pigments. J. Nat. Med. 74 (1), 1–16.
Matsui, K., Takaichi, S., Nakamura, M., 2003. Morphological and biochemical changes in carotenoid granules in the ventral skin during growth of the Japanese newt *Cynops pyrrhogaster*. Zool. Sci. 20 (4), 435–440.
Matsumoto, J., 1965. Studies on fine structure and cytochemical properties of erythrophores in swordtail, *Xiphophorus helleri*, with special reference to their pigment granules (Pterinosomes). J. Cell Biol. 27 (3), 493–504.
Meng, H., Shang, Y., Cheng, Y., Wang, K., Yu, J., Cao, P., Fan, S., Li, Y., Cui, J., 2021. Knockout of zebrafish colony-stimulating factor 1 receptor by CRISPR/Cas9 affects metabolism and locomotion capacity. Biochem. Biophys. Res. Commun. 551, 93–99.
Nagatsu, T., Ichinose, H., 1999. Regulation of pteridine-requiring enzymes by the cofactor tetrahydrobiopterin. Mol. Neurobiol. 19 (1), 79–96.
Pike, T.W., Blount, J.D., Bjerkeng, B., Lindström, J., Metcalfe, N.B., 2007. Carotenoids, oxidative stress and female mating preference for longer lived males. Proc. Biol. Sci. 274 (1618), 1591–1596.
Reboul, E., 2019. Mechanisms of carotenoid intestinal absorption: where do we stand? Nutrients 11 (4), 838.
Reboul, E., Abou, L., Mikail, C., Ghiringhelli, O., André, M., Portugal, H., Jourdheuil-Rahmani, D., Amiot, M.J., Lairon, D., Borel, P., 2005. Lutein transport by Caco-2 TC-7 cells occurs partly by a facilitated process involving the scavenger receptor class B type I (SR-BI). Biochem. J. 387 (Pt 2), 455–461.
Schmeisser, J., Verlhac-Trichet, V., Madaro, A., Lall, S.P., Torrissen, O., Olsen, R.E., 2021. Molecular mechanism involved in carotenoid metabolism in post-smolt Atlantic Salmon: Astaxanthin metabolism during flesh pigmentation and its antioxidant properties. Mar. Biotechnol. (NY) 23 (4), 653–670.
Sefc, K.M., Brown, A.C., Clotfelter, E.D., 2014. Carotenoid-based coloration in cichlid fishes. Comp. Biochem. Physiol. A. Mol. Integr. Physiol. 73C (100), 42–51.
Shiraki, T., Kojima, D., Fukada, Y., 2010. Light-induced body color change in developing zebrafish. Photochem. Photobiol. Sci. 9 (11), 1498–1504.
Shosuke, I., Wakamatsu, K., 1998. Chemical degradation of melanins: application to identification of dopamine-melanin. Pigment Cell Res. 11 (2), 120–126.
Sulliman, N.C., Ghaddar, B., Gence, L., Patche, J., Rastegar, S., Meilhac, O., Diotel, N., 2021. HDL biodistribution and brain receptors in zebrafish, using HDLs as vectors for targeting endothelial cells and neural progenitors. Sci. Rep. 11 (1), 6439.
Sušnik, B.S., Djurdjević, I., Linares, A.C., Kreft, M.E., 2022. Genetic and correlative light and electron microscopy evidence for the unique differentiation pathway of erythrophores in brown trout skin. Sci. Rep. 12 (1), 1015.
Tanaka, S., 2001. Endocrine mechanisms controlling body-color polymorphism in locusts. Arch. Insect Biochem. Physiol. 47 (3), 139–149.
Taxiarchis, A., Mahdessian, H., Silveira, A., Fisher, R.M., Van't-Hooft, F.M., 2019. PNPLA2 influences secretion of triglyceride-rich lipoproteins by human hepatoma cells. J. Lipid Res. 60 (6), 1069–1077.
Toomey, M.B., Lopes, R.J., Araújo, P.M., Johnson, J.D., Gazda, M.A., Afonso, S., Mota, P. G., Koch, R.E., Hill, G.E., Corbo, J.C., Carneiro, M., 2017. High-density lipoprotein receptor SCARB1 is required for carotenoid coloration in birds. Proc. Natl. Acad. Sci. U. S. A. 114 (20), 5219–5224.
Våge, D.I., Boman, I.A., 2010. A nonsense mutation in the beta-carotene oxygenase 2 (BCO2) gene is tightly associated with accumulation of carotenoids in adipose tissue in sheep (*Ovis aries*). BMC Genet. 11, 10.
Verwilligen-Robin, A.F., Mulder, L., Araújo, P.M., Carneiro, M., Bussmann, J., Hoekstra, M., Van, E.M., 2013. Zebrafish as outgroup model to study evolution of scavenger receptor class B type I functions. Biochim. Biophys. Acta Mol. Cell Biol. Lipids 1868 (6), 159308.
Vissio, P.G., Darias, M.J., Di-Yor, M.P., Pérez-Sirkin, D.I., Delgadin, T.H., 2021. Fish skin pigmentation in aquaculture: the influence of rearing conditions and its neuroendocrine regulation. Gen. Comp. Endocrinol. 301, 113662.
Vitt, S., Bakowski, C.E., Thünken, T., 2022. Sex-specific effects of inbreeding on body coloration and physiological color change in the cichlid fish *Pelvicachromis taeniatus*. BMC Ecol. Evol. 22 (1), 124.
Wang, C., Lu, B., Li, T., Liang, G., Xu, M., Liu, X., Tao, W., Zhou, L., Kocher, T.D., Wang, D., 2021. Nile Tilapia: a model for studying teleost color patterns. J. Hered. 112 (5), 469–484.
Wang, J.M., Liu, H.H., Ma, S.C., Xi, Y., Zhang, R.P., Xu, Q., Li, L., 2022. Progress on the formation mechanism of sexual dimorphism plumage color in birds. Hereditas 44 (6), 491–500.
Yamaguchi, Y., Hearing, V.J., 2014. Melanocytes and their diseases. Cold Spring Harb. Perspect Med. 4 (5), a017046.
Yan, Y., Chen, R., Wang, X., Hu, K., Huang, L., Lu, M., Hu, Q., 2019. CCL19 and CCR7 expression, signaling pathways, and adjuvant functions in viral infection and prevention. Front. Cell Dev. Biol. 7, 212.
Zemanová, L., Navrátilová, H., Andrýs, R., Šperková, K., Andrejs, J., Kozáková, K., Meier, M., Möller, G., Novotná, E., Šafr, M., Adamski, J., Wsól, V., 2019. Initial characterization of human DHRS1 (SDR19C1), a member of the short-chain dehydrogenase/reductase superfamily. J. Steroid Biochem. Mol. Biol. 185, 80–89.
Zhang, Y., Liu, J., Peng, L., Ren, L., Zhang, H., Zou, L., Liu, W., Xiao, Y., 2017. Comparative transcriptome analysis of molecular mechanism underlying gray-to-red body color formation in red crucian carp (*Carassius auratus*, red var.). Fish Physiol. Biochem. 43 (5), 1387–1398.